Journal of ELECTRONIC MATERIALS, Vol. 36, No. 12, 2007
DOI: 10.1007/s11664-007-0258-6

Special Issue Paper

Microstructural Aspects of Nucleation and Growth of (In,Ga)As-GaAs(001) Islands with Low Indium Content

V.P. KLADKO,[1] V.V. STRELCHUK,[1] A.F. KOLOMYS,[1] M.V. SLOBODIAN,[1] YU.I. MAZUR,[2,3] ZH.M. WANG,[2] VAS. P. KUNETS,[2] and G.J. SALAMO[2]

1.—Lashkaryov Institute of Semiconductor Physics, NAS of Ukraine, Prospekt Nauki 45, Kyiv 03028, Ukraine. 2.—Department of Physics, University of Arkansas, Fayetteville, Arkansas 72701, USA. 3.—e-mail: ymazur@uark.edu

Molecular beam epitaxy growth of multilayer $In_xGa_{1-x}As/GaAs(001)$ structures with low indium content (x = 0.20–0.35) was studied by X-ray diffraction and photoluminescence in order to understand the initial stage of strain-driven island formation. The structural properties of these superlattices were investigated using reciprocal space maps, which were obtained around the symmetric 004 and asymmetric 113 and 224 Bragg diffraction, and $\omega/2\theta$ scans with a high-resolution diffractometer in the triple axis configuration. Using the information obtained from the reciprocal space maps, the 004 $\omega/2\theta$ scans were simulated by dynamical diffraction theory and the in-plane strain in the dot lattice was determined. We determined the degree of vertical correlation for the dot position ("stacking") and lateral composition modulation period (LCM) (lateral ordering of the dots). It is shown that initial stage formation of nanoislands is accompanied by LCM only for [110] direction in the plane with a period of about 50 to 60 nm, which is responsible for the formation of a quantum wire like structure. The role of $In_xGa_{1-x}As$ thickness and lateral composition modulation in the formation of quantum dots in strained $In_xGa_{1-x}As/GaAs$ structures is discussed.

Key words: InGaAs, self-organized quantum dots, X-ray diffraction, photoluminescence

INTRODUCTION

Molecular-beam-epitaxy (MBE)-grown (In,Ga)As quantum dots (QDs) have attracted increasing attention for a basic understanding of heteroepitaxial growth as well as applications in new optoelectronic devices.[1,2] It is usually assumed that coherent (In,Ga)As islands are formed by the Stranski–Krastanow (S–K) mechanism, i.e., only after the formation of a two-dimensional (2D) elastically strained wetting layer (WL) of some critical thickness.[3] However, a number of recent studies[4–6] have shown that the conventional picture of S–K growth may be not too simple, and the growth mode may depend strongly on parameters such as substrate temperature, growth rate, V/III ratio,[3] In content,[7] and substrate misorientation.[8] Besides these parameters, which govern the island formation, intrinsic growth phenomena can occur. For instance, it is now recognized that surface segregation of indium leads to the structural and compositional modification of the WL and QDs.[9–11] In addition, under suitable growth conditions, spontaneous lateral composition modulation (LCM) can occur during the growth of III-V alloys[12] that may serve as a suitable template for 1D (quantum wire) and 0D (quantum dot) structures. As a result, during the deposition of InAs on GaAs there are often found to be nanoislands elongated along the $[1\bar{1}0]$ direction.[13,14] This is a well-known effect, and was studied in detail in Refs. 15 and 16. Recently, InAs QDs shape anisotropy along the $[1\bar{3}0]$ and $[3\bar{1}0]$

(Received April 3, 2007; accepted May 23, 2007; published online October 2, 2007)

directions was also observed.[17] The formation of such elongated islands was discussed theoretically by Tersoff and Tromp.[18]

Despite the large number of experimental and theoretical studies, the nature of the 2D → 3D transition is still of great interest and debate. One of the models by which self-assembled QDs can form was proposed by Priester and Lannoo.[19] They showed that for highly mismatched heteroepitaxy the existence of a narrow distribution of the size and shape in the dot population can be explained by the formation of stable 2D platelets with one monolayer (ML) height that act as precursors for the formation of 3D coherent islands. According to this mechanism, 2D platelets reach a critical coverage, where their repulsive interaction induces a spontaneous transformation into 3D islands with the same areal distribution. Scanning tunneling microscopy (STM) investigations of InAs/GaAs QDs reveal the existence of "quasi-3D islands" (2–4 ML high), which are an intermediate structure during the 2D → 3D transition.[13] A similar feature has also been observed for Ge-Si(001) islands.[20] A more recent STM study of the nucleation and growth of (In,Ga) As-GaAs(001) islands with low In content (0.25)[21] reveals islands in the initial stage of the 2D → 3D transition to be flat 2D platelets (1–3 ML high) elongated along $[\bar{1}10]$ with a length-to-width ratio of ~2. Moreover, it was shown that the overgrowth of QDs with a spacer layer can lead to a change in shape and local changes in the strain and composition.[22] To the best of our knowledge, there is no systematic investigation of structural changes that occur during the 2D → 3D transition in (In,Ga)As for MBE growth with a low In content.

The use of X-ray scattering techniques allows the nondestructive characterization of self-assembled semiconductor QDs.[23–25] Recently, we have studied the influence of In/Ga segregation and interdiffusion on the process of 2D → 3D transition in InGaAs/GaAs multilayer heterostructures using high-resolution X-ray diffraction and resonant Raman scattering.[16]

In this paper, we report on X-ray high-resolution reciprocal space mappings (HR-RSMs) and photoluminescence (PL) investigations of the 2D → 3D transition in 8-fold $In_xGa_{1-x}As$/GaAs (001) with low In content. The study of X-ray diffuse scattering using HR-RSMs allows us to investigate both lattice and morphological imperfections of a material. It has been shown that the change in the spatial distribution of the deformations in the epitaxial layers due to the presence of QDs strongly influences the spatial distribution of the scattered X-ray intensity. Also, it has been found that under these growth conditions the formation of the InGaAs islands is accompanied by lateral composition modulation in $In_xGa_{1-x}As$ layers along the [110] direction on the GaAs(001) surface.[26] This is because of the anisotropic diffusion of adatoms due to the dimerization of the As-stabilized GaAs surface. As a result, the two surface directions, i.e., [110] and $[1\bar{1}0]$, are not equivalent even for an ideal flat surface free from monolayer steps. This fact can be used to obtain arrays of spatially ordered nanoislands in the form of QD chain stacks without using a template substrate.[13,27]

EXPERIMENT

The growth of $In_xGa_{1-x}As$/GaAs QD multilayers was carried out in a commercial solid-source Riber-32 MBE system equipped with reflection high-energy electron diffraction (RHEED). So-called "epi-ready" semi-insulating GaAs (001) substrates were loaded into the MBE growth chamber. After the surface oxide layer was removed, a 0.5-μm-thick GaAs buffer layer was grown at 580°C with a growth rate of 1.0 monolayer per second (ML/s). During the growth of all the samples, the As_4 beam equivalent pressure (BEP) from a valve-controlled cell was kept constant at 1×10^{-5} Torr. The substrate temperature was reduced to 520°C for the growth of five complete sets of samples with eight periods of the $In_xGa_{1-x}As$ (14 ML)/GaAs (70 ML) structure. While the nominal layer thickness of these samples was constant, the nominal In compositions were 0.20, 0.25, 0.28, 0.30 and 0.35. The In composition variation for different sample sets was achieved by performing the $In_xGa_{1-x}As$ growth with the In flux corresponding to a 0.2 ML/s growth rate and the Ga flux adjusted by changing the Ga source temperature. The QD nucleation was seen directly by reflection high energy electron diffraction when the pattern changed from streaky to spotty. We observed three-dimensional island formation after $In_xGa_{1-x}As$ deposition of 14.0 ML, 10.7 ML and 7.4 ML for samples with In content of 0.28, 0.30 and 0.35, respectively. For $x = 0.20$ and 0.25, no QD formation was found. Surface morphological information was obtained from atomic force microscopy (AFM) (in contact mode) of the last but uncapped QD layer.

The PL measurements were performed in a variable temperature (5–300 K) He cryostat under the excitation of a continuous wave Ar^+-laser with a wavelength of 488 nm. The PL signals from the samples were analyzed using a 0.5 m spectrometer and the spectra were recorded using a standard lock-in technique and a liquid-N_2-cooled Ge detector.

Rocking curves were measured by high-resolution "Philips X'Pert PRO MRD XL" diffractometer with a Bartel's four-crystal Ge monochromator using CuK_a radiation. Three-crystal Ge(220) analyzer with 12 arcsec angular divergence was used to obtain the reciprocal space maps. For all the samples the reciprocal space maps (RSM) were measured in symmetric 004 and asymmetric 113 and 224 diffraction geometries (glancing incidence angles). Rocking curves and RSMs were measured for various azimuthal directions. The diffraction plane was (110) and $(1\bar{1}0)$ for 004, 113 and 224 geometries. The

miscut angle of the (001) substrate is smaller than 0.5°. The simulation on the basis of various models was performed to extract the structural characteristics and the strain field distribution from the observed patterns.[16]

EXPERIMENTAL RESULTS

The energy-level structure and geometry of QDs were monitored using PL and AFM, respectively. Figure 1a displays a PL spectra (T = 300 K) of $In_xGa_{1-x}As/GaAs$ structures with various nominal In concentrations, obtained under weak excitation. For the samples with x = 0.20 and 0.25 pseudomorphic 2D growth mode is realized and PL spectrum for each sample consists of single intensive band due to emission from $In_xGa_{1-x}As$ quantum wells (QWs). These PL bands are centered at 1.295 eV and 1.259 eV with a full width at half maximum (FWHM) of 9 and 18 meV for the samples with x = 0.20 and 0.25, respectively. The low-energy shift, while QW thickness remains, has been attributed to the increasing In concentration in QW. Small FWHM of this PL band demonstrates the high structural quality of the QW. The presence of negligible tail at the high-energy side of the PL band can be attributed to thermally activated processes of carrier trapping to parts of the QW with higher potential, which occur due to monolayer fluctuations of thickness and local variations in In content[28] Energy position of $In_xGa_{1-x}As/GaAs$ QW PL band is in agreement with the results of Ref. 29.

However, for $x > 0.25$ an abrupt change in spectral emission is observed (Fig. 1). As can be seen from the Fig. 1a, for the sample with x = 0.28 a dramatic increasing of FWHM of the PL band as well as shift to lower energy takes place. The PL spectrum reflects the distribution of the QD energy levels.

Another noteworthy feature of the low-power PL spectra for the x = 0.28 sample is its doublet character with 49 meV energy spacing.[30] In agreement with our AFM images of the uncapped $In_{0.28}Ga_{0.72}As$ QDs (Fig. 1b) this doublet is likely caused by different island sizes. In this case the islands are well separated (Fig. 1b) and no coupling is expected.

HR-RSM measurements were made on this multilayer sample to investigate the variations in the lateral structure. The sample was rotated while the detector was fixed at a position corresponding to the (004), (113) and (224) diffraction peak of the GaAs substrate. In this configuration, the scanning path in reciprocal space is parallel to the sample surface. HR-RSMs were obtained in two mutually perpendicular lateral directions [110] and [1$\bar{1}$0] by rotating the sample through 90° in a plane parallel to its surface. Figure 2 shows 113 HR-RSMs obtained from the samples with In content 0.20, 0.25, 0.28 and 0.35, illustrating the initial stage of nanoislands nucleation and growth. Measured maps reveal sharp maxima at $q_x = 0$, which are designated as SL_0 and $SL_{\pm1}$ and present the distribution of coherently scattered intensity. Horizontal widths of these peaks are determined by diffractometer resolution. Coherently scattered waves depend only on laterally averaged sample structure. It is interesting to point out that on the maps obtained for (1$\bar{1}$0) diffraction plane, which is perpendicular to the [1$\bar{1}$0] direction, the broadening of maxima and thickness fringes are observed. This indicates that there is lateral lattice tilt along the defined directions.

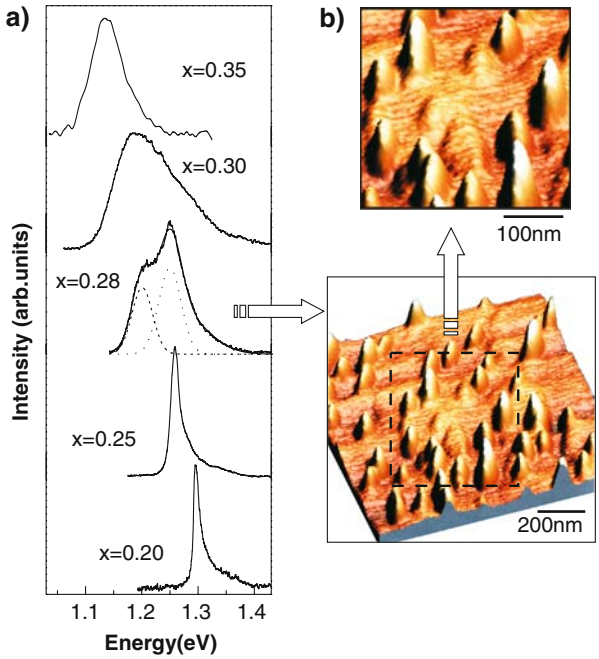

Fig. 1. (a) Normalized PL spectra of the multilayer $In_xGa_{1-x}As/GaAs(001)$ structures with different In content measured at T = 300 K, (b) AFM images of the grown QDs upon $In_xGa_{1-x}As$ layers with a nominal In concentration of 0.28.

Peaks on Figs. 2 and 4, marked as S correspond to the diffraction from the substrate, where SL_n is the n-th satellite peak, of a laterally averaged superlattice (SL). The distance between satellites equals $2\pi/D$ (D is the SL period) while the distance between SL_0 and substrate peak is proportional to the difference between substrate vertical lattice parameter and average SL parameter.

It is well-known that self-organized quantum dots generate X-ray diffuse scattering (XDS), which follows the coherent diffraction.[23] XDS is caused by the difference in InAs and GaAs scattering factors and the elastic deformation field in GaAs matrix around the dots. In this case the diffuse scattering mostly arises from the deformation field both outside and inside the dot. XDS intensity distribution in the q_x direction is also determined by lateral ordering of the QDs, which causes the appearance of lateral satellites in the $q_x = 2\pi p/L$ (where L is the average distance between dots and p is an integer) positions. The distance between lateral satellites is $2\pi/L$ and their width is proportional to the disper-

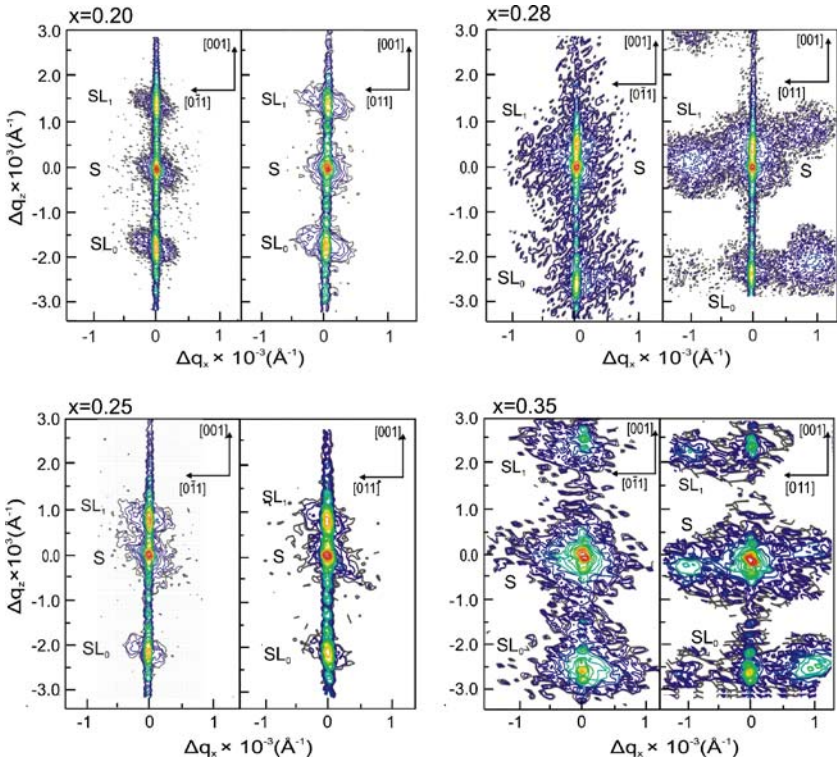

Fig. 2. High-resolution reciprocal space maps of the multilayer InGaAs/GaAs structures measured in asymmetrical 113 geometry for (1$\bar{1}$0) (left column) and (110) (right column) diffraction planes.

sion of the distance distribution. Samples with low In content ($x \leq 0.25$) show no anisotropic correlated roughness, suggesting that some minimum concentration of In is required to produce the correlated wavy morphology.

The information about QDs is contained in the diffuse peaks, which accompany the coherent satellites.[23] On the maps, obtained in asymmetrical diffraction geometry, the diffuse peaks are asymmetrical relative to the q_z axis, which is clearly observed in the cross-sectional line scans along the q_x direction (Fig. 3). In the vicinity of SL_0 (i.e. for low value of $|q|$ vector) the diffuse scattering is determined mostly by the deformation field and the lattice scattering factor at a distance from a dot. A diffuse intensity maximum around SL_0 is shifted in the positive q_x direction, which corresponds to the compressive deformation ε in GaAs matrix between dots. On the other hand the diffuse peaks around SL_1 are shifted in negative q_x direction. Therefore this part of the diffuse scattering results from expanded lattice regions, i.e. from the dots volume.

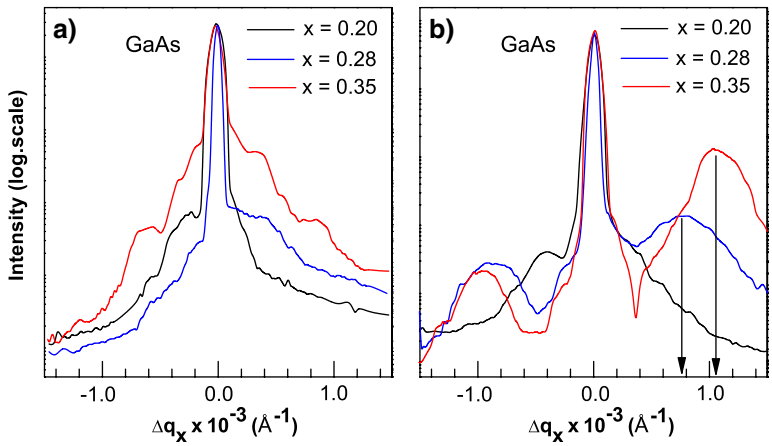

Fig. 3. Projection of the diffuse peaks around SL_0 satellite on the q_x axis determined from the measured reciprocal space maps (Fig. 2), around the 113 reciprocal-lattice point for the multilayer InGaAs/GaAs structure and for diffraction plane (1$\bar{1}$0) (a) and (110) (b). The solid arrows show the lateral satellites due to the in-plane ordering of the dot positions.

Table I. Parameters of Multilayer $In_xGa_{1-x}As/GaAs$ Structures Obtained from X-ray Measurements

Composition	*D*, nm	ε GaAs	ε InGaAs	*L*, nm	σ, nm
0.20	21.7 ± 0.7	–0.00018	0.00047	–	–
0.25	21.9 ± 0.3	–0.00018	0.00026	–	–
0.28	22.2 ± 0.6	–0.00030	0.0034	62 ± 2	15 ± 6
0.30	22.4 ± 0.1	–0.00025	0.0040	55 ± 2	17 ± 7
0.35	22.9 ± 0.7	–0.00036	0.0044	51 ± 2	18 ± 7

An average deformation, average lateral distance between dots, and its statistical dispersion were estimated and are presented in Table I.

Figure 3 presents the q_x projection of diffuse peaks near SL_0 obtained in the asymmetrical 113 geometry for the samples with an In content of 0.20, 0.28 and 0.35. Lateral maxima appear only for the (110) scattering surface and only one of them is observed, while the others are suppressed because of the large dispersion σ (σ—dispersion of lateral distance between QDs). It should be noted that in the case of symmetrical 004 diffraction lateral maxima are also observed (not shown here) in spite of the short coherence length of the incident X-ray wave. It is, also important to mention that the diffuse maxima are absent for the $(1\bar{1}0)$ incidence plane for all samples.

Analogous diffuse maxima for the (110) scattering surface are also observed in q_x projection near SL_1 satellite (Fig. 4). It has to be pointed out that the positions of lateral satellites for 113 and 224 reciprocal lattice points are identical, which corresponds to the same homogeneity degree of QDs in the growth direction.

DISCUSSION

At present, no complete explanation exists for the nature of strained epitaxy and the kinetics that are responsible for the formation of quantum wire-like structures and especially its anisotropy. PL and AFM analysis for the sample with a nominal In content of 0.28 gives us an opportunity to state that for the initial stage of 2D-3D transition two types of quantum structure are formed: In enriched 3D-like islands which correspond to the low-energy emission peak in PL and 2D-like islands with smaller In concentration which are characterized by small height and comparatively large lateral size (possibly in the form of 2D-platelets[19,21]). The latter are responsible for the high-energy component of PL band and they can be considered as precursors of large 3D-like islands.

For the samples with $x = 0.30$ and $x = 0.35$ the critical thickness for the 2D-3D transition reduces to 10.7 ML and 7.4 ML, respectively, while islands surface density increases.[16] The islands have an elliptic base with main and secondary axes oriented along $[1\bar{1}0]$ and [110] surface directions, respectively. When x is increased from 0.30 to 0.35 the average lateral size of the island changes from 42 nm to 35 nm along $[1\bar{1}0]$ direction and from 22 nm to 15 nm along [110] direction. In all the cases island height did not exceed about 1 nm. We did not observe the phenomenon of dot coalescence or large island formation with edge dislocations, which can be due to the inhomogeneous distribution of In and Ga atoms in InGaAs wetting layer. The absence of these effects is due to the In segregation and lateral compositional modulation.

The presence of pronounced asymmetry in the X-ray diffuse peaks for various diffraction planes, i.e. $(1\bar{1}0)$ and (110), indicates that the lateral satellites are caused by composition modulation in determined crystallographic directions.

From the satellite width $\delta Q_x = (\sigma \cdot Q_x)^2/L$ the root mean square dispersion σ of the distance between dots was estimated.[31] The value $L/\sigma \approx 3 \pm 1$ for the samples with In content 0.30–0.35 demonstrates that the dots position is correlated up to the third-order neighbor, i.e. only short range lateral ordering takes place.

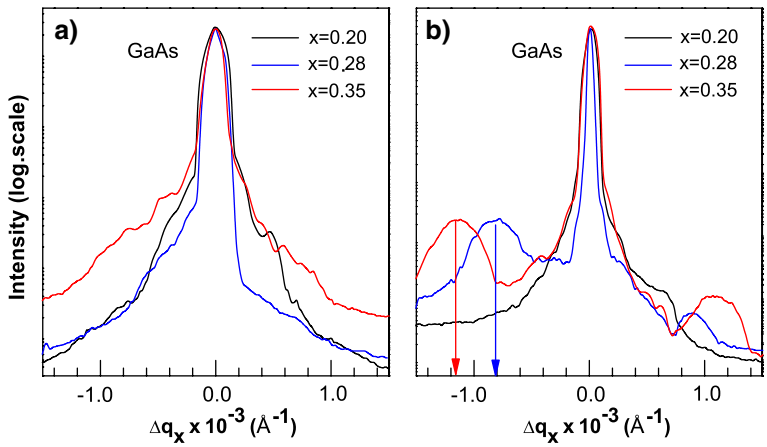

Fig. 4. High-resolution coplanar diffraction around 113 reciprocal-lattice point from multilayer InGaAs/GaAs structure and for diffraction planes $(1\bar{1}0)$ (a) and (110) (b). Shown scans present the integrated intensity from area scan (Fig. 2) along SL_1 satellite.

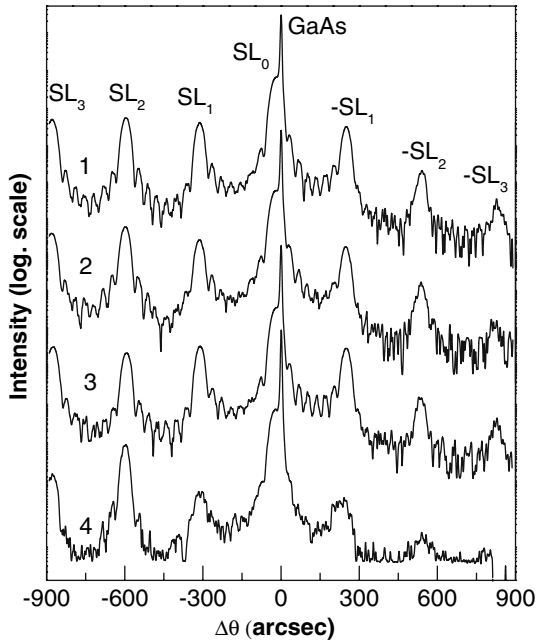

Fig. 5. Cross-sectional line scans along the q_z direction obtained from HR-RSMs near the 004 reciprocal lattice point for multilayer InGaAs/GaAs structures (sample with a nominal In concentration of 0.28) and different q_x. The distance between two nearby scans is $\delta q_x = 0.1$ reciprocal lattice units.

It is well known that the dots' vertical ordering influences the diffuse maxima width in q_z direction.[23] These widths can be seen on the Fig. 5 where linear q_z scans are presented measured in the vicinity of 004 Bragg peak for various q_x values. From Fig. 5 one can see that in our case the width of satellites' diffuse maxima does not depend on the satellite order. Coherent widths in our measurements are nearly $2\pi/(ND)$, where N is the number of periods. We estimated the vertical correlation length $\xi_{cor}/(ND) > 0.65$, and made the conclusion that more than 65% of the dots are vertically correlated.

CONCLUSIONS

In summary, we have investigated the formation of quantum dots in the very early stages of the growth process for multilayer $In_xGa_{1-x}As/GaAs$ structures with (x = 0.20–0.35).

AFM and PL results showed that for low strain ($x < 0.25$) no direct evidence of 3D growth is seen. For larger x it was shown by AFM that $In_xGa_{1-x}As$ islands are elliptically shaped and that the major and minor axes of islands are along the [1$\bar{1}$0] and [110] directions, respectively. Elongated islands' shape is attributed to anisotropy of the diffusion length for adatoms along different crystallographic directions and the minimization strain energy of the whole system.

The results of our experimental and theoretical X-ray data analysis confirm that the multilayer $In_xGa_{1-x}As/GaAs$ structures are of good quality. The interface between barrier GaAs and $In_xGa_{1-x}As$ QWs with In content 0.20–0.25 is sharp and coherent. Further, increasing the In concentration in the $In_xGa_{1-x}As$ alloy leads to the appearance of lateral composition modulation with further formation of 2D-like dimensional nanoislands. This lateral composition modulations and the lateral ordering of nucleation sites for the nanoislands occurs in the rigorously defined crystallographic [110] directions and could be related to a preferred direction of strain relaxation.

Thus, our observation of one-dimensional periodic lateral structures converted from a $In_xGa_{1-x}As/GaAs$ multilayers with $x > 0.25$ could suggest a new way for making quantum wires and chains of QDs[32] grown by MBE.

REFERENCES

1. P. Bhattacharya, S. Ghosh, and A.D. Stiff-Roberts, *Annu. Rev. Mater. Res.* 34, 1 (2004).
2. V.M. Ustinov, A.E. Zhukov, A.Yu. Egorov, and N.A. Maleev, *Quantum Dot Lasers* (N.Y.: Oxford University Press, 2003).
3. D. Bimberg, M. Grundmann and N. N. Ledensov, *Quantum Dot Heterostructures* (Wiley & Sons, 1999).
4. P.B. Joyce, T.J. Krzyzewski, G.R. Bell, B.A. Joyce, T.S. Jones, *Phys. Rev. B* 58, R15981 (1998).
5. G. Medeiros-Ribeiro, A.M. Bratkovski, T.I. Kamins, D.A.A. Ohlberg, and R.S. Williams, *Science* 279, 353 (1998).
6. M. Henini, *Nanoscale Res. Lett*. 1, 32 (2006).
7. M.Ya. Valakh, V.V. Strelchuk, A.F. Kolomys, Yu.I. Mazur, Zh.M. Wang, M. Xiao, and G.J. Salamo, *Semiconductors* 39, 127 (2005).
8. N. Ikoma and S. Ohkouchi, *Jpn. J. Appl. Phys.* 34, L724 (1995).
9. N. Grandjean, J. Massies, and O. Tottereau, *Phys. Rev. B* 55, R10189 (1997).
10. B. Shin, B. Lita, R.S. Goldman, J.D. Phillips, and P.K. Bhattacharya, *Appl. Phys. Lett.* 81, 1423 (2002).
11. Y.H. Chen, X.L. Ye, and Z.G. Wang, *Nanoscale Res. Lett.* 1, 79 (2006).
12. R.D. Twesten, D.M. Follstaedt, S.R. Lee, E.D. Jones, J.L. Reno, J.M. Millunchick, A.G. Norman, S.P. Ahrenkiel, and A. Mascarenhas, *Phys. Rev. B* 60, 13619 (1999).
13. R. Heitz, T.R. Ramachandran, A. Kalburge, Q. Xie, I. Mukhametzhanov, P. Chen, and A. Madhukar, *Phys. Rev. Lett.* 78, 4071 (1997).
14. P. Podemski, R. Kudrawiec, J. Misiewicz, A. Somers, J.P. Reithmaier, and A. Forchel, *Appl. Phys. Lett.* 89, 061902 (2006).
15. V.V. Strelchuk, P.M. Lytvyn, A.F. Kolomys, M.Ya. Valakh, Yu.I. Mazur, Zh.M. Wang, and G.J. Salamo, *Semiconductors* 41, 73 (2007).
16. Yu.I. Mazur, Zh.M. Wang, G.J. Salamo, V.V. Strelchuk, V.P. Kladko, V.F. Machulin, M.Ya. Valakh, and M.O. Manasreh, *J. Appl. Phys.* 99, 023517 (2006).
17. A. Michon, I. Sagnes, G. Patriarche, G. Beaudoin, M.N. Mèrat-Combes, and G. Saint-Girons, *Phys. Rev. B* 73, 165321 (2006).
18. J. Tersoff and R.M. Tromp, *Phys. Rev. Lett.* 70, 2782 (1993).
19. C. Priester and M. Lannoo, *Phys. Rev. Lett.* 75, 93 (1995).
20. F.M. Ross, R.M. Tromp, and M.C. Reuter, *Science* 286, 1931 (1999).
21. S.O. Cho, Zh.M. Wang, and G.J. Salamo, *Appl. Phys. Lett.* 86, 113106 (2005).
22. O. Kirfel, E. Muller, D. Grutzmacher, and K. Kern, *Physica E* 16, 602 (2003).
23. M. Schmidbauer, *X-ray Diffuse Scattering from Self-Organized Mesoscopic Semiconductor Structures, Springer*

Tracts in Modern Physics, Vol. 199. (Berlin: Springer, 2004), p. 204.
24. V.V. Strelchuk, V.P. Kladko, O.M. Yefanov, O.I. Gudymenko, M.Ya. Valakh, A.F. Kolomys, Yu.I. Mazur, Zh.M. Wang, and G.J. Salamo, *Semiconductor Phys., Quantum Electronics & Optoelectronics* 8, 35 (2005).
25. D. Grigoriev, M. Schmidbauer, P. Schäfer, S. Besedin, Yu.I. Mazur, Zh.M. Wang, G.J. Salamo, and R. Köhler, *J. Phys. D: Appl. Phys.* 38, A154 (2005).
26. E. Penev, P. Kratzer, and M. Scheffler, *Phys. Rev. B* 64, 085401 (2001).
27. P. Sutter and M.G. Lagally, *Phys. Rev. Lett.* 84, 4637 (2000).
28. A. Gustafsson, M.-E. Pistol, L. Montelius, and L. Samuelson, *J. Appl. Phys.* 84, 1715 (1998).
29. Yung-Hui Yeh and Joseph Ya-min Lee, *J. Appl. Phys.* 81, 6921 (1997).
30. G. Saint-Girons and I. Sagnes, *J. Appl. Phys.* 91, 10115 (2002).
31. A.A. Darhuber, P. Schittenhelm, V. Holy, J. Stangl, G. Bauer, and G. Abstreiter, *Phys. Rev. B* 55, 15652 (1997).
32. Zh.M. Wang, Yu.I. Mazur, G.J. Salamo, P.M. Lytvyn, V.V. Strelchuk, and M.Ya. Valakh, *Appl. Phys. Lett.* 84, 4681 (2004).